Stochastic Modelling and Computational Sciences
Vol. 1 No. 1 (June, 2021)

Received: 01st March 2021 *Revised: 08th May 2021* *Accepted: 04th June 2021*

A CFD Approach Toward Simulation of Flow Distribution in Shell & Tube Heat

P. S. Mak, Dept. of Industrial and Manufacturing System Engg., The university of Hong Kong, Hong Kong

Abstract

Non-uniform flow distribution from header to the branch pipes in a flow system will lead to 25% decrease in effectiveness of a cross flow heat exchanger [4]. Both analytical and experimental approach reported so far is applicable to a limited number of engineering applications. This simulation study is an attempt to illustrate how Computational Fluid Dynamics (CFD) software can be an effective tool for filling up the requirement. The predicted results are compared with the available experimental data to validate the CFD procedure. The effect of various parameters on flow distribution in a flow system is also investigated. The present approach can be adopted for any flow system including Shell and Tube heat exchangers.

1. INTRODUCTION

Heat Exchangers as Economizers in Boilers, as air-cooled liquid sodium heat exchanger by natural convection in Nuclear Reactors, etc., have a flow system consisting of two headers (manifolds) and connecting coils (laterals/branch pipes) in between. Inlet header is a dividing flow type and the outlet header is a combining flow type as shown in Fig 1.1. One of the common assumptions while designing the heat exchanger is that, the flow is distributed uniformly through the dividing headers. The design procedure starts with simple assumptions like header diameter and the inlet nozzle diameter to header etc., which are to be fine-tuned further based on the experience gained. Due to these assumptions, practically mal distribution is common and significantly reduces the desired performance of the equipment.

Keywords: Flow distribution, Mal distribution, Header, Computational Fluid Dynamics (CFD).

AMS: Applied Mathematics–Computational Mathematical applications in Fluid Dynamics.

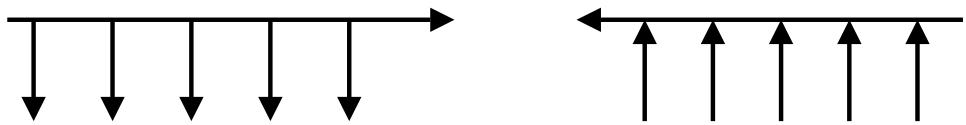

Fig 1.1: Schematic representation of Dividing and Combining flow Headers

Analytical method for designing a header has been proposed by London et al. [5] and Bajura R. A [2]. Modeling of a header requires determination of both axial and lateral velocities and the static pressure distributions. Two basic approaches such as analytical and numerical methods are reported widely for header design of flow systems. Bajura R. A. and Jones E.H [3] have published analytical solution for one-dimensional mathematical model based on Navier Stokes equation as well as experimental data for dividing & combining header of parallel and reverse flow system. Majumdar [6] has solved one-dimensional continuity and momentum equations by Finite Volume Method for flow system analysis of dividing and combining headers. Calculations based on one dimensional flow equation from orifice equation, fanning equation and momentum balance equation were carried out for dividing and combining headers having constant cross section by Acrivos A et al. [1].

Sachiyo Horiki et al. [9] have derived the applicable equations from Bernoulli's theorem with the introduction of friction loss coefficient, pressure regain coefficient and inlet distribution loss coefficient for closed end of headers. Many researchers have adopted the same coefficients in various forms for their mathematical models. Zhengqing Miao and Xu Tongmo [11] have published one-dimensional mathematical model for headers and three-dimensional mathematical model for branch pipes from the first principles, and applied to seven different flow systems by considering super heater of a boiler. Experimental results are available for total flow system in few literatures like Bajura R.A. and Jones E.H [3]. The flow distribution mechanism of water in a horizontal thin square header with four vertical pipes (with or without a gas phase) have been studied by Osakabe Masahiro et al [8], and the iterative calculation procedure for the design has been recommended for a single-phase condition in a dividing header with water stagnant condition at one end. All these mathematical models are one-dimensional only.

Mueller A.C. and Chiou J.P [7] reviewed various factors affecting flow distribution inside a shell and tube heat exchanger, without any mathematical model or experimental data. An attempt to study flow system in a shell and tube heat exchanger is reported by Lalot et al. [4], in which the experiments were conducted

in a graphite block, having perpendicular drilled passages with electric heaters in one passage, and air in another passage to simulate the condenser environment. The correlations obtained from the experimentation have been applied to the heat exchangers and reported effectiveness variation for different velocity ratios (maximum to minimum velocity across the heat exchanger). Yanzhong Li and Zhe Zhang [10] have optimized the channel flow distribution by modifying the inlet header configuration of a plate-fin heat exchanger using CFD. Flow distribution in tube side of the shell and tube heat exchanger is varying widely from the above certified literatures in fluid entry, tube arrangement etc.

Systematic study on various kinds of headers and flow systems necessitates a common platform usage, which can reduce the experimental set up cost and increase the data availability for any type of geometric configuration of the total flow system. With the availability of high-speed computers, CFD analysis can be a better alternative to assess the performance of the flow system. The purpose of the study is to get reliable results as that of the experimentation with a relatively low cost and lesser time. This work involves CFD simulation, validation and to understand the impact of the geometrical variations in a header over the flow distribution in the total system like non uniform lateral spacing.

2. GOVERNING EQUATIONS AND CFD PROCEDURE

CFD software called FLUENT was used to simulate the fluid flow and the pressure distribution in various flow systems. The flow systems were modeled three dimensionally and meshed in to finite volumes. The meshed model was then imported in to CFD software for analysis. To predict the properties of the given turbulent flow with no prior knowledge of turbulent structure, Standard k-μ model is chosen in addition to the mass conservation and momentum equations. The Standard k-ε model is basically a two-equation model based on transport equations for the turbulence kinetic energy (***k***) and its dissipation rate (ε) as given below:

$$\frac{\partial}{\partial t}(\rho k)+\frac{\partial}{\partial x_i}(\rho k u_i)=\frac{\partial}{\partial x_j}\left[\left(\mu+\frac{\mu_t}{\sigma_k}\right)\frac{\partial k}{\partial x_j}\right]+G_k+G_b-\rho\varepsilon-Y_m+S_k$$

and,

$$\frac{\partial}{\partial t}(\rho\varepsilon)+\frac{\partial}{\partial x_i}(\rho\varepsilon u_i)=\frac{\partial}{\partial x_j}\left[\left(\mu+\frac{\mu_t}{\sigma_\varepsilon}\right)\frac{\partial \varepsilon}{\partial x_j}\right]+C_{1\varepsilon}\frac{\varepsilon}{K}(G_k+G_b)-C_{2\varepsilon}\rho\frac{\varepsilon^2}{k}+S_\varepsilon$$

In these equations, $\boldsymbol{G_k}$ represents the generation of turbulence kinetic energy due to the mean velocity gradients, $\boldsymbol{G_b}$ is the generation of turbulence kinetic energy due to buoyancy, $\boldsymbol{Y_M}$ represents the contribution of the fluctuating dilatation in compressible turbulence to the overall dissipation rate, $C_{1\varepsilon}$, $C_{2\varepsilon}$, and $C_{3\varepsilon}$ are closure coefficients. σ_k and σ_ε are the turbulent Prandtl numbers for k and ε respectively. S_k and S_ε are user-defined source terms. The values for the closure coefficients are given as:

$$C_{1\varepsilon} = 1.44,\ C_{2\varepsilon} = 1.92,\ \sigma_k = 1,\ \sigma_\varepsilon = 1.3$$

The segregated solver based on implicit approach was chosen to solve the above equations. A first order upwind differential scheme was initially applied for differencing of momentum, turbulence kinetic energy and turbulence dissipation rate. Discretisation scheme for pressure is STANDARD and pressure velocity coupling is through SIMPLE algorithm. As air is drawn from the atmosphere to circulate through the flow system in experimentation (Bajura R.A. and Jones E.H [3]), Hydraulic diameter and medium turbulence intensity are the inputs for the turbulent model. Under Relaxation factors are suitably set to converge the results in a better way. The numerical simulation errors such as truncation and round off errors are limited by specifying the convergent condition to absolute residuals less than 10^{-6}. Boundary conditions specified are: velocity of the fluid at the inlet of the dividing header and pressure was specified at the outlet of the combining header. The wall of the header was assumed to be at no slip condition and the fluid is air.

3. EVALUATION OF MAL DISTRIBUTION

The mass flow rate through the individual outlets of the dividing header, across its cross section is accounted through surface integration, to predict the difference in flow rate as the mal distribution using the formula:

$$m_i = (M_i - M_a)/M_a$$

4. FLOW DISTRIBUTION MODELS

The symmetric model of the dividing header in a shell and tube heat exchanger with number of branch outlet stubs is shown in the Fig 4.1. To these outlet stubs, coils of the heat exchanger are connected, which carries the fluid for heat transfer. The tube side fluid has to enter through a 5 cm diameter inlet nozzle of the dividing header and after getting distributed, the fluid has to leave through coils. At the end of coils again a similar header of the combining type is available to collect the fluid, which in turn leaves through a 5 cm diameter outlet nozzle. Total flow system

in three dimensional shown in Fig. 4.2 has to be analysed for variation in flow rates through branch pipes, which is not covered in the previous investigations.

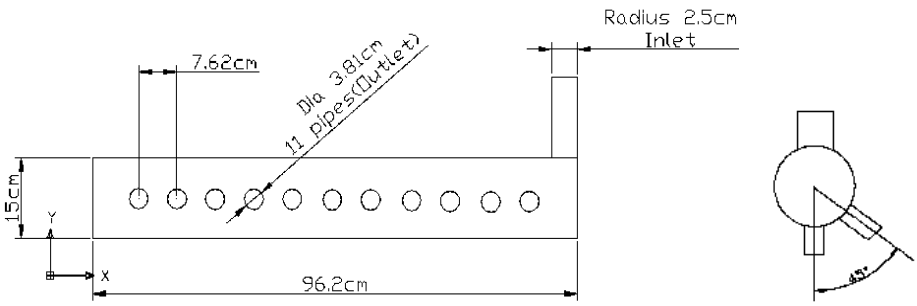

Fig. 4.1: 2D Model of the Header used for CFD analysis

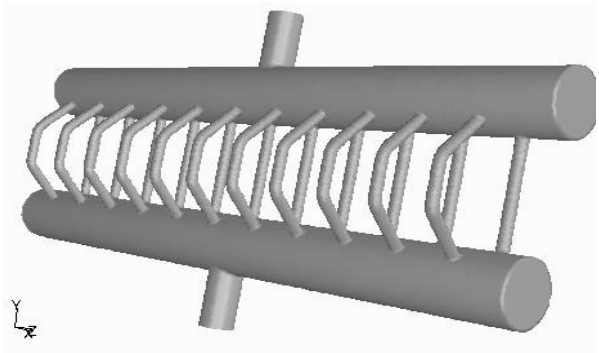

Fig. 4.2: 3D Model of the Header used for Shell and Tube type heat exchanger

To adopt a suitable procedure in CFD for the above model, experimental data published by Bajura R.A. and Jones E.H [3] was chosen, whose two dimensional experimental setup grid diagram is shown in the Fig.4.3. The headers and the laterals are having diameters of 10.16 cm and 3.81 cm respectively. Parallel and reverse flow systems were arranged by capping one end of the dividing header accordingly. The spacing between the laterals is uniform at 2.55 times the header diameter. Each header was instrumented by pressure taps located mid way between the branch points. Orifices of two different internal diameters were inserted at the midpoint of the laterals to increase the flow resistance. Tests were conducted with either 20 or 10 branch pipes depends on the case. The same experimental conditions were incorporated in the CFD analysis.

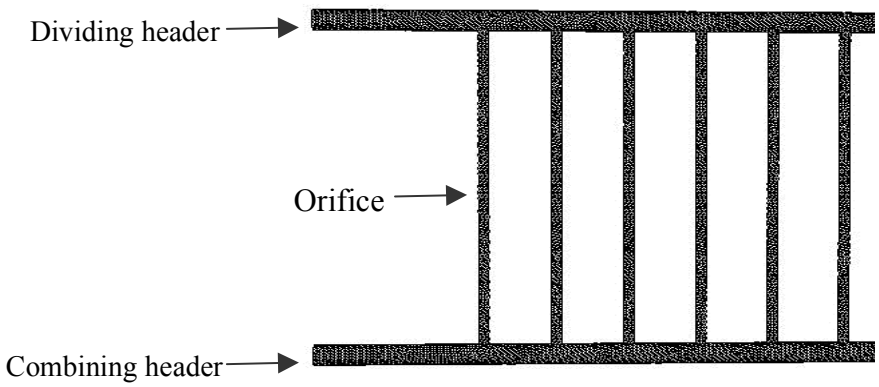

Fig. 4.3: Schematic Grid diagram of the Experimental system of Bajura and Jones[3]

5. RESULTS AND DISCUSSION

Bajura R.A. and Jones E.H. [3] conducted experiments for four major cases. In each case the experiments were conducted for reverse and parallel flow systems as shown in Fig. 5.1 and the results were plotted as dimensionless pressure with respect to the dimensionless distance of the branch pipes from the inlet.

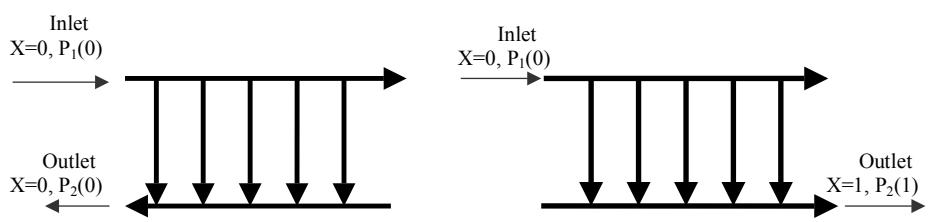

Fig.5.1: Schematic representation of Reverse and Parallel Flow System

In case of Parallel flow systems,

$$\text{Dimensionless Pressure} = \frac{P_i - P_2(1)}{\Delta P_r}$$

where, $\Delta P_r = P_1(0)-P_2(1)$.

In case of Reverse flow systems,

$$\text{Dimensionless Pressure} = = \frac{P_i - P_2(0)}{\Delta P_r}$$

where, $\Delta P_r = P_1(0)-P_2(0)$.

Case A: This case consists of 20 lateral pipes with large area ratio (A_r), 2.810 having a large lateral flow resistance created by an orifice of diameter 2.54 cm, located in the middle of the branch pipe. The flow in the dividing header is dominated by the effects of static pressure regain due to the drop in velocity as the fluid leaves through the successive branch points. After a branch point, in the straight portion of the header the fluid experiences a pressure drop due to friction. The net pressure difference available just before each branch point determines the flow quantity through that branch pipe. In combining header, when fluid enters it accelerates the mainstream fluid and decreases the pressure along the flow direction.

In parallel flow arrangement, the flow enters the dividing header with an initial pressure, whereas the corresponding point of the combining header will also have a higher pressure due to the accumulation of the fluid at the capped end. The differential pressure will be lower at that point compared to the differential pressure of the combining header outlet end. In summary, a higher differential pressure variation along the flow direction is observed in the parallel flow system. But a completely opposite trend is observed in case of a reverse flow system because the inlet point of the dividing header is rearranged.

The pressure characteristics of each header in the reverse flow system are better matched to provide a more uniform discharge than the parallel flow system. The same physics is observed in the CFD analysis of the model, which is reflected in terms of dimensionless pressure versus dimensionless distance as shown in Fig. 5.2.

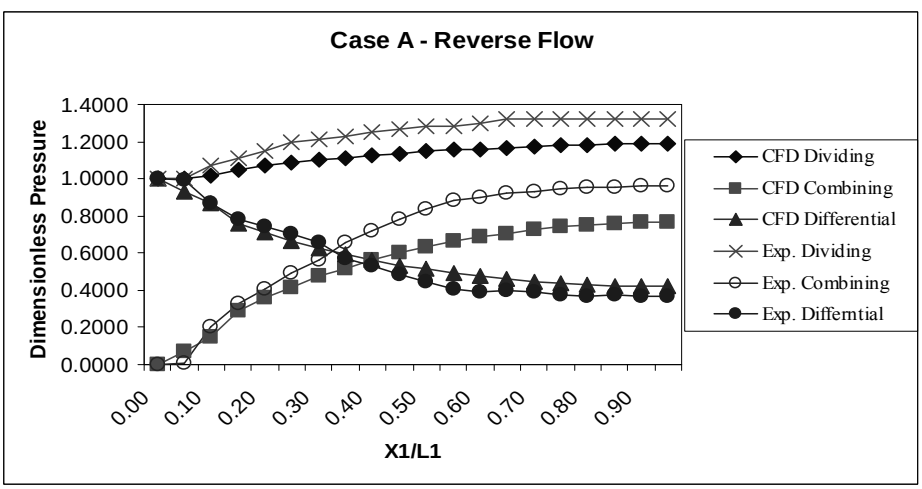

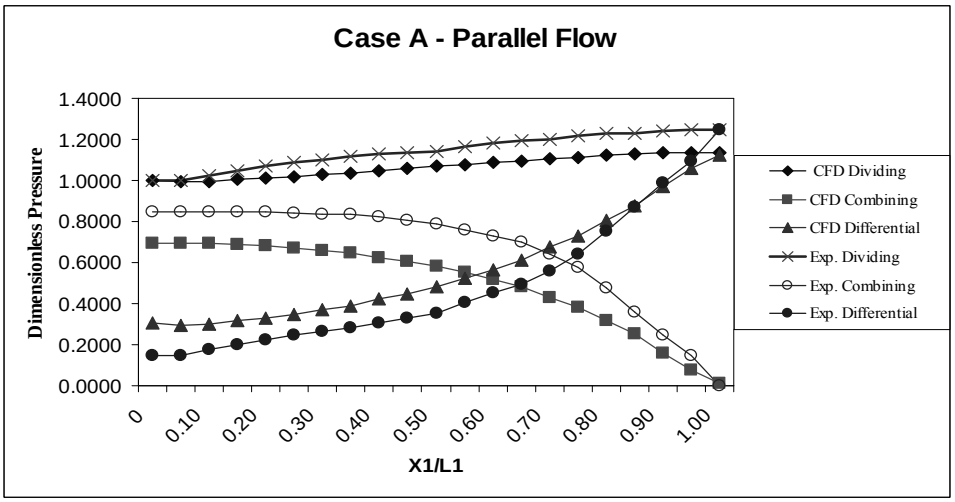

Fig. 5.2: Experimental and CFD results of Pressure profiles for Case A

Case B: This case differs from case A in orifice diameter (3.18 cm) introduced at the middle of the branch pipes. It reduces the lateral flow resistance and causes a poor flow distribution in each system, however the reverse flow manifold still exhibits a better flow balance due to the matched pressure characteristics of the header. The published experimental results and the CFD analysis results are compared in Fig. 5.3.

Case C: This case is with a smaller area ratio of 1.405 and 50% header length of Case A & B due to reduction in number of branch pipes (10 nos.). The larger

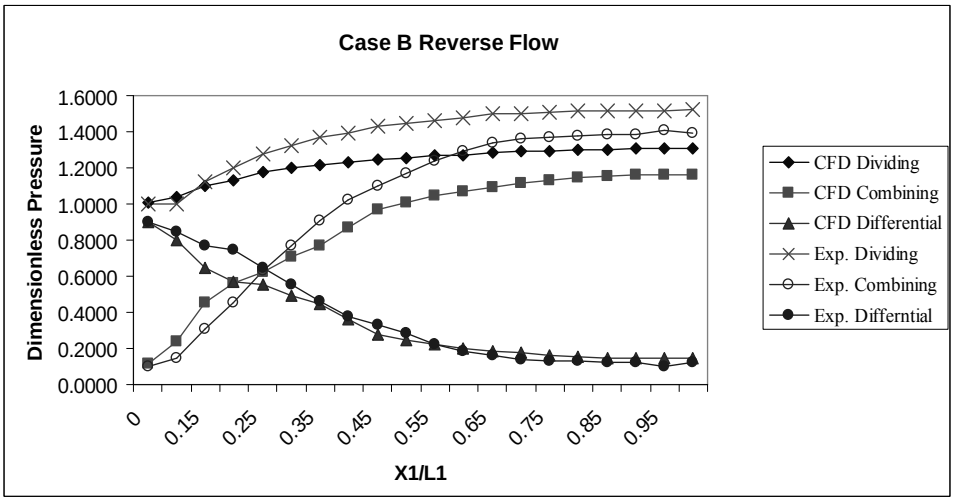

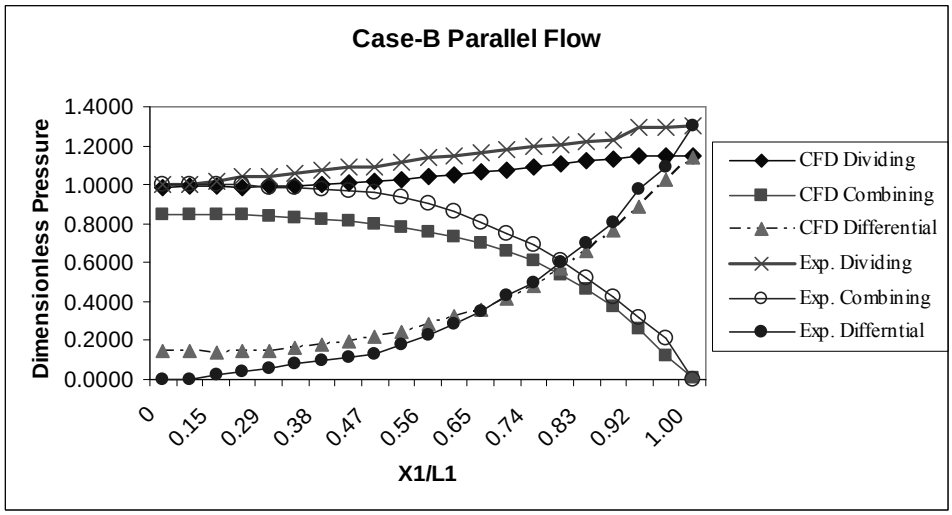

Fig. 5.3: Experimental and CFD results of Pressure profiles for Case B

lateral flow resistance was created with an orifice diameter of 2.54 cm introduced in the middle of the lateral pipes. The flow distribution is nearly uniform due to the large flow resistance of the laterals and the small area ratio. The comparison of the published experimental results and CFD analysis results is shown in Fig. 5.4.

Case D: This case differs from Case C in which the smaller lateral resistance is created with an orifice of diameter 3.18 cm. The flow distribution was much poorer than Case C due to the smaller lateral resistance. The experimental data and the CFD analysis results comparison is presented on Fig. 5.5.

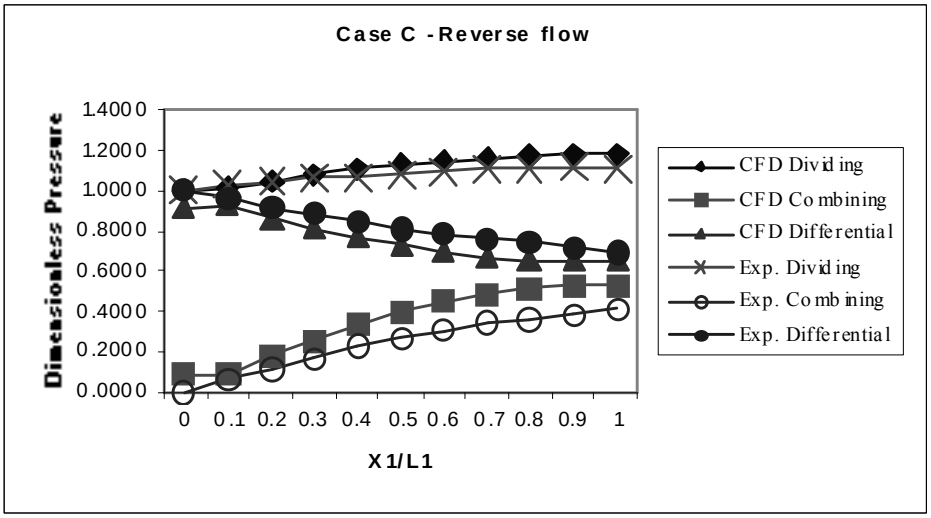

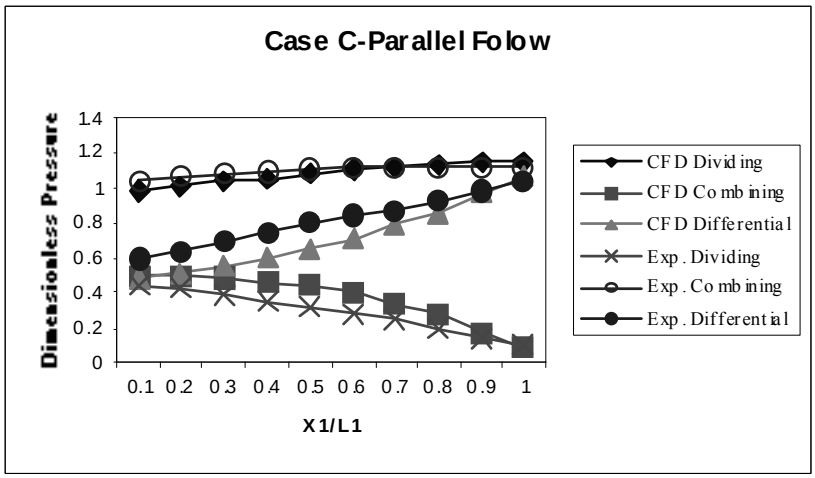

Fig. 5.4: Experimental and CFD results of Pressure profiles for Case C

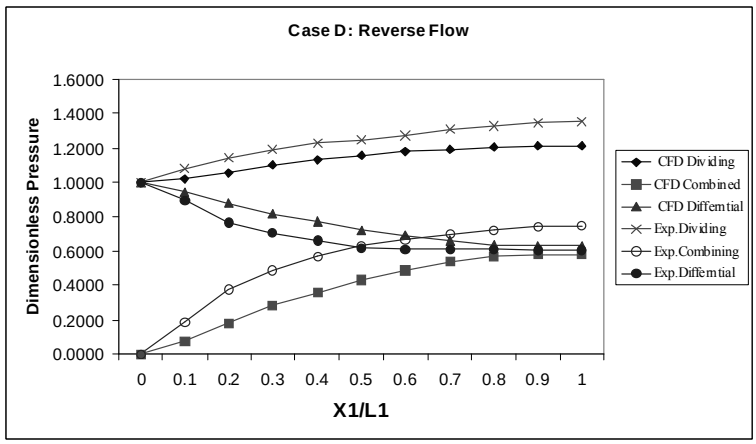

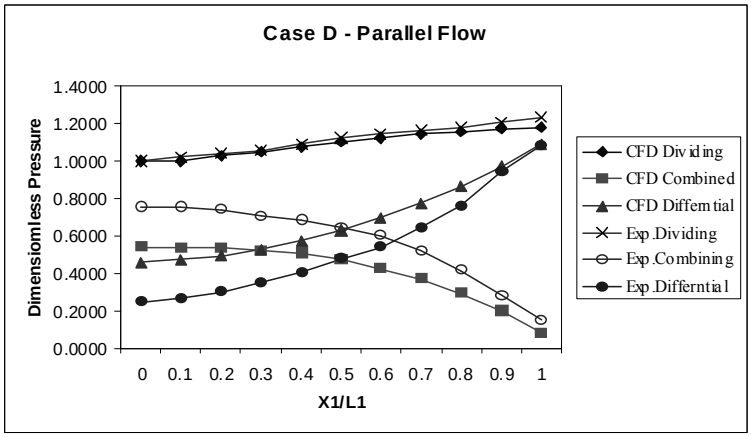

Fig. 5.5: Experimental and CFD results of Pressure profiles for Case D

The result patterns obtained in all the cases were qualitatively similar to that of the experimental one. The error magnitude was found to be less than 20%. The reasons for the error is as explained below:

The location of the blower and its characteristics in the experimental setup is not clearly mentioned in the literature and hence its effect is not included in the CFD model. In addition, numerical computation errors are accountable.

The mal distribution based on the flow rates is extracted from the predicted data for both the flow systems. The mal distribution in the reverse flow system is almost negligible when compared to the parallel flow system due to a smaller differential pressure variation along the flow direction. In reverse flow system the differential pressure variation along the flow direction is almost linear, whereas in the parallel flow system it is exponential. The same is reflected in the mal distribution graph shown in Fig. 5.6. The branch pipe numbering (outlet in the abscissa of the graph) is from the inlet end of the header towards the laterals in the flow direction.

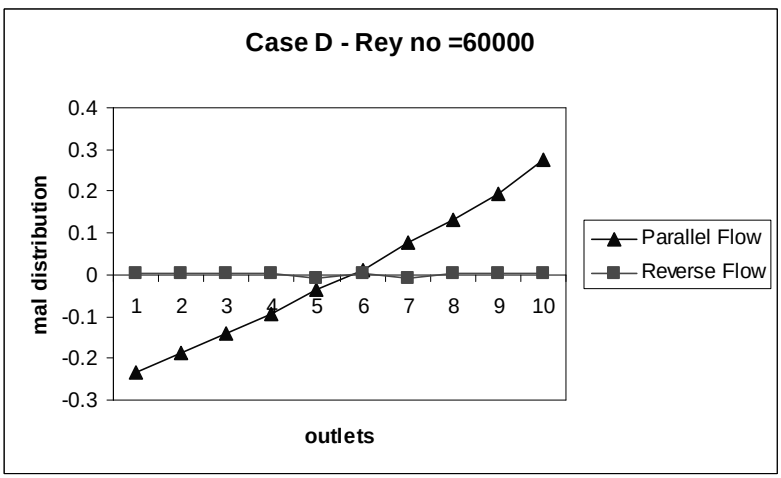

Fig. 5.6: Mal Distribution in the Reverse flow and Parallel flow systems for Case-D

5.1. Effect of Fluid Properties on Mal Distribution:

In the experimental study, the fluid used was air, but for the heat exchangers in Nuclear reactors and Boilers, the fluid used is normally liquid sodium and water. Hence a comparative study was done between air, and the other two liquids at elevated temperatures in case D of Bajura R.A. and Jones E.H [3]. This gives an idea about the operability of other fluids in the same flow system.

The properties of the two fluids applied are:

- Water at Temperature-220^{0}c:

  Density = 584 kg/m^3, Kinematic Viscosity = 0.149x10^{-6} m^2/s,

- Liquid Sodium at Temperature–500^{0}c:

  Density=829 kg/m^3, Kinematic Viscosity= 0.289x10-^{6} m^2/s.

The Reynolds number maintained in the inlet header for all the fluids was same and equal to 60,000. The effect of heat transfer on flow distribution is not included in the present study though the fluid is at elevated temperature since a negligible heat transfer to the surrounding from the heat exchanger is a common design assumption. The results are shown in the Figures 5.7 & 5.8. The mal distribution trend is similar for all the three fluids, increasing linearly from the nearest pipe to that of the farthest from the inlet. Also the mal distribution for air and water are similar and higher in magnitude, whereas in liquid sodium it is relatively small.

The differential pressure distribution along the flow direction is similar in pattern and magnitude for air and water, whereas the liquid sodium exhibits a different behavior.

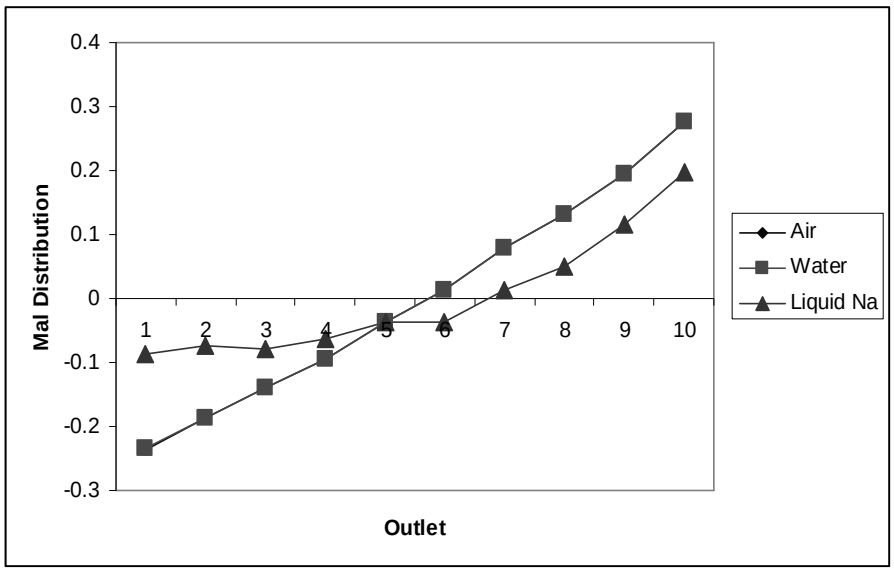

Fig. 5.7: Comparison of Mal Distribution for Different Fluids for Case-D

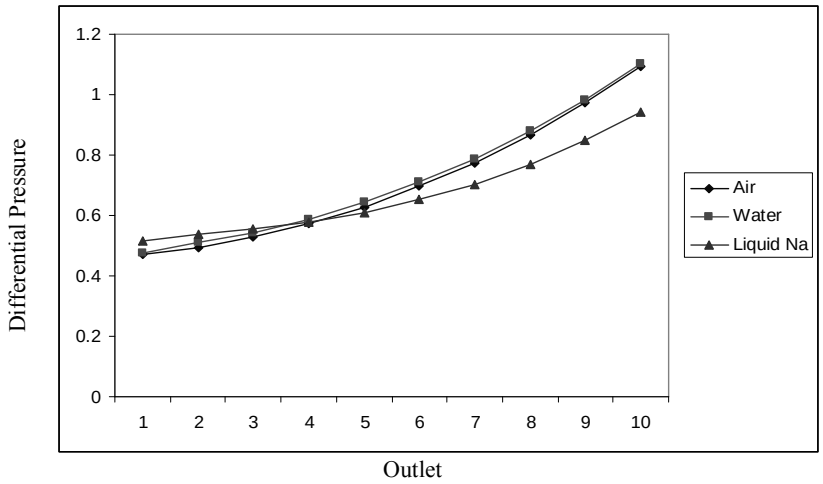

Fig. 5.8: Comparison of Differential Pressure in Flow System for Different Fluids for Case-D

5.2. Effect of Lateral Spacing on Mal Distribution

In mathematical models and experimental studies, the uniform lateral spacing is normally studied. The lateral spacing is varied in case D of Bajura R.A. and Jones E.H [3] and its impact on mal distribution are plotted as shown in Fig.5.9. For the incremental case, spacing between consecutive laterals was incremented in an arithmetic progression with 0.1 times the header diameter as common difference, as well as decremented in the same way for the other case and results are plotted. Mal distribution is comparatively lower in case of the equal lateral spacing than the other two cases, which are almost similar.

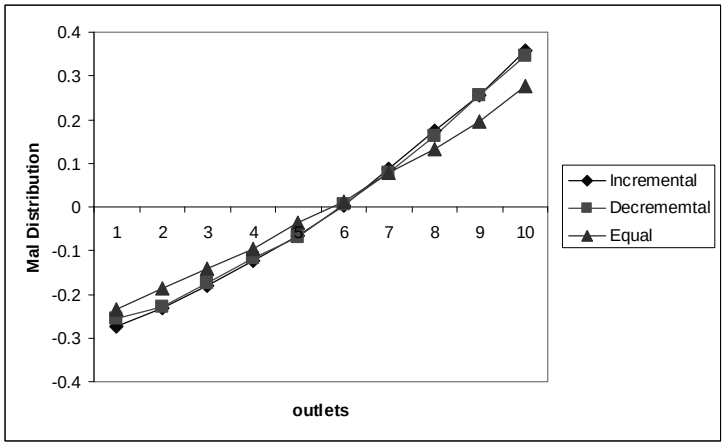

Fig. 5.9: Effect of Lateral Spacing on Flow Distribution

5.3. Flow Mal distribution in a Shell and tube heat exchanger flow system:

After CFD procedure validation against experimental data, the flow distribution in the shell and tube heat exchanger flow system (as shown in the Fig. 4.2) is predicted. The results obtained from the analysis are plotted as shown in Fig. 5.10. The mal distribution in the outlet branch pipes positioned nearer to the inlet nozzle is maximum, which is due to a higher-pressure difference, and it reduces for the farther pipes due to the pressure regaining effect. The branch pipe numbering (outlet in the abscissa of the graph) is from the inlet nozzle to right hand side. Also a comparative study was made between different turbulent models impact on the predicted results namely Standard k- ε, RNG k-ε (based on re-normalization group theory) and Realizable k-ε. All these three models have shown almost similar behavior to predict the flow distribution.

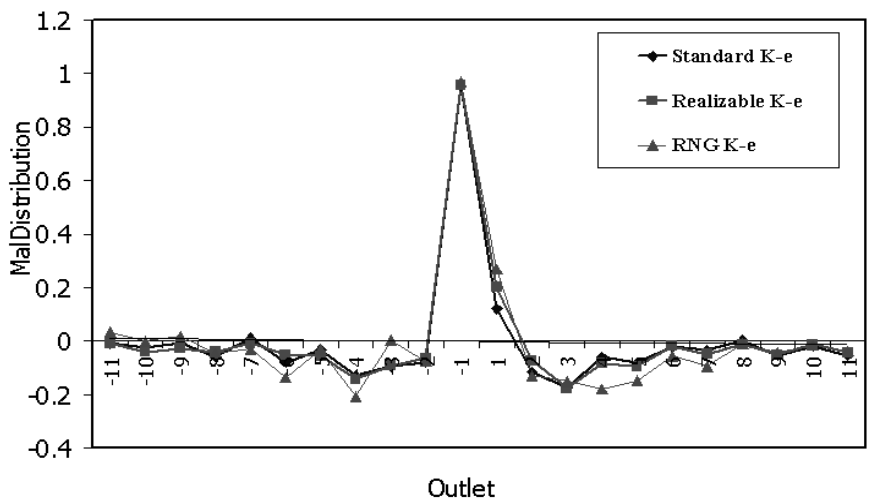

Fig. 5.10: Flow Distribution in a Shell and Tube heat Exchanger for Different Turbulent Models

6. CONCLUSIONS

- To validate the CFD procedure followed for a shell and tube heat exchanger flow system, available experimental data from the literature were compared with predicted results.
- The numerical analysis was able to capture the physics reported in the referred literatures such as pressure recovery in the flow direction of a dividing header, the opposite phenomena in the combining header and the reverse flow observed near the last branch point of the combining header outlet.

- The maximum mal distribution was observed in the branch pipes, which are against inlet nozzle of the dividing header in the shell and tube heat exchanger flow system from the CFD analysis. The same pattern has been verified by field temperature measurements i.e maximum temperature of the fluid is observed at the mal distribution identified branch points.
- Out of the numerical data from CFD analysis, generation of the coefficients such as pressure regain coefficient, inlet distribution loss coefficient versus various flow ratios (lateral pipe flow rate/header inlet flow rate) is possible for different flow systems. The coefficients will be helpful in extending the available mathematical models to other flow system configurations.
- The practical application also requires the study of multiphase fluid flow distribution, which can be a future scope of the study.

REFERENCES

[1] Acrivos, A., Babcock, B. D., and Pigford, R. L., Flow distribution in manifolds, Chemical Engineering Science, **10** (1959), 112-124.

[2] Bajura, R.A., A model for flow distribution in manifolds, ASME *Journal of Engineering Power,* **93** (1971), 7-12.

[3] Bajura, R.A., and Jones, E.H., Flow distribution manifolds, ASME *Journal of Fluid Engineering,* **98** (1976), 654-666.

[4] Lalot, S., Florent, P., Lang, S.K., and Bergles, A.E., Flow mal-distribution in heat exchangers, *Applied Thermal Engineering,* **19** (1999), 847-863.

[5] London, A.L., Klopfer, G., and Wolf, S., Oblique flow headers for heat exchangers, ASME *Journal of Engineering Power,* **90** (1968), 45-56.

[6] Majumdar, A.K., Mathematical Modeling of Flows in Combining and dividing flow manifolds, *Applied Mathematical Modeling,* **4** (1980), 424-432.

[7] Mueller, A. C., and Chiou, J. P., Review of various types of flow mal-distribution in heat exchangers, *Heat Transfer Engineering,* **9** (1988), 36-50.

[8] Osakabe Masahiro, Tomoyuki Hamada, and Sachiyo Horiki, Water flow distribution in header contaminated with bubbles, *International Journal of Multiphase Flow,* **25** (1999), 827-840.

[9] Sachiyo Horiki, Tomoshige Nakamura, and Masahiro Osakabe, Thin Flow Header to Distribute Feed Water for Compact Heat Exchanger, Experimental Thermal and Fluid Science, **28** (2004), 201-207.

[10] Yanzhong, Li., and Zhe Zhang, CFD simulation on inlet configuration of plate-fin heat exchangers, Cryogenics **43** (2003), 673-678.

[11] Zhengqing Miao, and Xu Tongmo, Single phase flow characteristics in the headers and connecting tubes of parallel tube platen systems, Applied Thermal Engineering, **26** (2006), 396-402.

Nomenclature

A_r	Area Ratio = (no. of lateral pipes x cross section area of a lateral pipe)/ Area of the header
L_1	Total length of the Header (m)
m_i	Mal Distribution
M_i	Mass flow rate through individual branch pipes (kg/s)
M_a	Average mass flow rate through the branch pipes (kg/s)
$P_1(0)$	Pressure at the inlet Dividing header (Pa)
$P_2(0)$	Pressure at the outlet of the Combining header in a reverse flow system (Pa)
$P_2(1)$	Pressure at the outlet of the Combining header in a parallel flow system (Pa)
P_i	Pressure at corresponding branch point (Pa)
Re	Reynolds number
u	Fluid Velocity (m/s)
X_1	distance of the branch point from the fluid entry point (m)
k	Turbulent kinetic energy (m^2s^{-2})
ε	Rate of dissipation of turbulent kinetic energy (m^2s^{-2})
ρ	Density of the fluid (kgm^{-3})